J. Membrane Biol. 171, 195–207 (1999)

The Journal of
Membrane
Biology

Glycosylation Influences Voltage-Dependent Gating of Cardiac and Skeletal Muscle Sodium Channels

Y. Zhang[1], **H.A. Hartmann**[2], **J. Satin**[1]

[1]Department of Physiology, University of Kentucky College of Medicine, Lexington, KY 40536-0298, USA
[2]Department of Molecular Biology and Biophysics, Baylor College of Medicine, One Baylor Plaza, Houston, TX 77030, USA

Received: 8 April 1999/Revised: 18 June 1999

Abstract. The role of glycosylation on voltage-dependent channel gating for the cloned human cardiac sodium channel (hH1a) and the adult rat skeletal muscle isoform (μl) was investigated in HEK293 cells transiently transfected with either hH1a or μl cDNA. The contribution of sugar residues to channel gating was examined in transfected cells pretreated with various glycosidase and enzyme inhibitors to deglycosylate channel proteins. Pretreating transfected cells with enzyme inhibitors castanospermine and swainsonine, or exo-glycosidase neuroaminidase caused 7 to 9 mV depolarizing shifts of $V_{1/2}$ for steady-state activation of hH1a, while deglycosylation with corresponding drugs elicited about the same amount of depolarizing shifts (8 to 9 mV) of $V_{1/2}$ for steady-state activation of μl. Elevated concentrations of extracellular Mg^{2+} significantly masked the castanospermine-elicited depolarizing shifts of $V_{1/2}$ for steady-state activation in both transfected hH1a and μl. For steady-state activation, deglycosylation induced depolarizing shifts of $V_{1/2}$ for hH1a (10.6 to 12 mV), but hyperpolarizing shifts for μl (3.6 to 4.4 mV). Pretreatment with neuraminidase had no significant effects on single-channel conductance, the mean open time, and the open probability. These data suggest that glycosylation differentially regulates Na channel function in heart and skeletal muscle myocytes.

Key words: Ion channels — Glycosylation — Activation — Inactivation — Patch-clamp — Heart

Correspondence to: J. Satin

Introduction

The voltage-gated sodium channel mediates the rapid influx of sodium that occurs in most excitable tissues during the rising phase of the action potential. This establishes cell excitability and maintains the conduction properties in heart, skeletal muscle, and neuronal tissues. Sodium channels are heavily glycosylated integral membrane proteins (Barchi, Cohen & Murphy, 1980; Miller, Agnew & Levinson, 1983). About 20–30% of the molecular weight of the rat brain and skeletal muscle sodium channels is carbohydrate (Messner & Catterall, 1985). However, only about 5% of the molecular mass of the rat cardiac sodium channels is carbohydrate (Cohen & Barchi, 1993). Of the carbohydrate residues about half are sialic acid residues. The highest concentration of consensus glycosylation sites of the sodium channels are located in the S_5–S_6 linker of domain I (Catterall, 1992, Gellens et al., 1992). It is unclear what the physiological role of the sugar residues are for sodium channel function, and if the difference in the degree of glycosylation between the cardiac and noncardiac sodium channel isoforms affects the channel gating differently.

The general role of the glycosylation of membrane proteins is considered to be involved in the protein folding, sorting and membrane targeting (West, 1986; Bradshaw, McAlister-Henn & Douglas, 1988; Matter & Mellman, 1994; Schelffele, Peranen & Simons, 1995). Removal of sialic acid residues has acute, functional effects on Ca channels (Fermini & Nathan, 1991). However, whether sugar residues also affect the voltage-dependent channel gating for different sodium channel isoforms is still poorly understood. The large number of charged sialic acid residues on sodium channels raises the possibility that charged sugar residues may electrostatically interact with the channel. Changes in external

surface charges associated with the channel protein or adjacent membrane lipids could influence the electric field in the region of the channel voltage sensor and thus elicit a shift of the voltage dependence of channel gating (Hanck & Sheets, 1992; Hille, 1992). Multivalent cations added to channels reconstituted in a neutral bilayer shifted steady-state activation and inactivation voltage dependencies consistent with charges on the channel protein itself (Worley et al., 1992). Since sialic acid residues are negatively charged at physiological pH, a cloud of negative charges close to the sodium channel may be capable of reducing the local potential drop sensed by the voltage sensor of the channel. The result of such an effect is that a smaller depolarizing step is necessary for opening a given fraction of channels (Hille, 1992).

Treatment of eel electroplax or rat skeletal muscle sodium channels (μl) with neuraminidase to strip the negatively charged sialic acid from outside of the channel protein caused a large depolarizing shift of steady-state activation (Recio-Pinto et al., 1990; Bennett et al., 1997). Because of the different levels of glycosylation as well as the possibly structural differences of the channel proteins between human cardiac Na channel (hH1a) and skeletal muscle sodium channels (μl), we explored and compared the effects of decreasing sugar residues on the voltage dependent channel gating in these two sodium channel isoforms.

In the present study, we pretreated the cloned cardiac sodium channel (hH1a) and skeletal muscle isoform (μl), each heterologously expressed in the same mammalian cell line, with glycosidase or enzyme inhibitors to evaluate the contribution of sugar residues to the voltage dependence of channel gating. Under our control conditions, the cardiac channel in heterologous expression systems gate similarly to native cardiac preparations (Satin et al., 1992). In parallel, the μl current expressed in the HEK293 cells gates similarly to that in native tissues (Chahine et al., 1994; Wang, George & Bennett, 1996); this is in contrast to μl current expressed in *Xenopus* oocytes (Trimmer et al., 1989). We found that treatments designed to remove, or prevent addition of sugar residues had similar effects on steady-state voltage dependence of activation for the cardiac or skeletal muscle channels. To study the possible surface charge effect of sugar residues, we evaluated the effects of deglycosylation with increased external magnesium (Mg^{2+}). Mg^{2+} can alter the negative external surface potential mainly, but not exclusively, by screening the fixed negative charge (Hanck & Sheets, 1992). We found that deglycosylation of channel proteins with either glycosidase or enzyme inhibitors caused similar depolarizing shifts of the voltage dependence for steady-state activation of both hH1a and μl through removal of negative surface charges, whereas removal of sugar residues induced quite a different effect on the voltage dependence of steady-state inactivation and the macroscopic inactivation kinetics in hH1a and μl.

Materials and Methods

Heterologous Expression System: Transient Transfection of hH1a or μl cDNA in HEK293 Cells

Transient transfection was used to express hH1a or μl cDNA in HEK293 cells, which is a transformed human cell line stably expressing a SV40 T-antigen. Previous data showed that μl sodium channels expressed in mammalian CHO (Bennett et al., 1997) or HEK293 cells (Ukomadu et al., 1992) were glycosylated as those in native tissues (Gordon et al., 1988). Although the levels of glycosylation in heterologously expressed channels are less than those from native preparations (Gordon et al., 1988; Cohen & Levitt, 1993; Elmer et al., 1985), the robust expression level and native gating properties of sodium channels expressed in mammalian cells indicate that full glycosylation patterns are not necessary for functional sodium channels (Bennett et al., 1997; Ukomadu et al., 1992). Therefore, we expressed hH1a and μl in HEK293 cells in this study. The HEK293 cells were grown in high-glucose (4.5 mg/ml) Dulbecco's modified Eagle's medium (DMEM), supplemented with 2 mM L-glutamine, 10% fetal bovine serum, and 5 μg/ml of gentamicin (GIBCO) in a humid atmosphere incubator (37°C) supplied with 5% CO_2 and 95% O_2. Transfection of HEK293 cells grown to ~60% confluence on a 35 × 10-mm cell culture dish with 2 μg of plasmid DNA encoding either hH1a or μl with a standard calcium phosphate method. To increase the probability for identifying the expressed cells, 2 μg of plasmid DNA encoding green fluorescence protein (GFP) was cotransfected. For patch-clamping experiments, the cells were used 48 to 72 hr post-transfection.

Expression Constructs of hH1a and μl

The full length μl cDNA was ligated into the expression vector RBG4 at the EcoRI site (kindly provided by Dr. J. Kyle, University of Chicago). A full length hH1a cDNA was also inserted into a mammalian expression vector, and verified by restriction analysis. The full length GFPS65T cDNA was ligated into the expression vector Pci (a gift from Dr. T. McClintock, University of Kentucky), and the plasmid GFP was then used to cotransfect the HEK293 cells.

Deglycosylation of Sodium Channels

To remove the sialic acid residues from the transfected sodium channels, the exoglycosidase neuraminidase type X (Sigma) was used to pretreat the transfected cells at 0.15 U/ml (800 U per mg of protein) for 5 hr at 37°C before the recording. Castanospermine (Sigma) and swainsonine (Sigma) inhibit the enzymes involved in the early and late steps of N-linked glycosylation and thus prevent the addition of carbohydrates to channel protein. Castanospermine and swainsonine were used to pretreat the transfected cells at the concentrations of 100 μg/ml (0.53 mM/L) and 500 ng/ml (0.29 μM/L) respectively for 48 hr at 37°C before the patch-clamp studies. Drugs were washed out immediately prior to recording with solutions listed below.

Electrophysiological Recording

Solutions

For whole-cell recording, the bath solution contained (in mM): NaCl 120; KCl 5; $CaCl_2$ 0.1; $MgCl_2$: 1.0; CsCl 15; Tetraethylammonium

chloride (TEA): 10; Dextrose: 10; Hepes: 10, pH 7.4 with CsOH. The pipette solution contained (in mM): NaCl 10; CsCl: 132; $MgCl_2$: 1; EGTA: 3; Hepes: 10, pH 7.38 with CsOH. For cell-attached recording, the depolarizing bath solution contained (in mM): KCl 140; $CaCl_2$; $MgCl_2$ 1; EGTA: 10; Dextrose: 10; Hepes; 10 (pH = 7.4 with CsOH). The pipette (extracellular) solution is (in mM): NaCl 140; $CaCl_2$: 0.1; $MgCl_2$ 1; Tetraethylammonium chloride (TEA): 10; Hepes: 10, pH 7.4 with CsOH.

Voltage-Clamp Methods

Patch electrodes were made from borosilicate glass (Warner Instrument) and coated with Sylgard (Dow-Corning, Midland, MI) to minimize the capacitance of electrodes. A Model P-97 micropipette puller (Sutter Instrument) was used to pull the electrodes. Macroscopic sodium currents from cells transiently transfected with ether hH1a or μl were recorded using the whole-cell configuration of the patch-clamp technique. The electrodes filled with intracellular solution have resistances ranging from 1.5 to 2.0 MΩ. Voltage command pulses are generated by a microcomputer using pCLAMP software (v 6.03, Axon Instruments, Foster City, CA). Recorded currents were filtered at 10 kHz (−3 dB). An Axopatch 200 patch-clamp amplifier was used with series resistance compensation to about 80%. Single-channel recording was performed using the cell-attached patch-clamp configuration. The electrodes for cell-attached patch recordings had resistance in bath solution of about 2.0 MΩ. The data for single channel recording were filtered at 2.0 kHz (−3 dB). The leak and capacitive current were subtracted from the raw data either using the P/4 protocol for whole cell recordings or by subtracting averages of traces without channel activity for single channel recordings.

A 1 to 1.5 mV time-dependent, hyperpolarizing shifts of the voltage dependence of steady-state activation and inactivation was observed, every 10 minutes during 1 hr of whole-cell recording for μl and hH1a (*data not shown*), consistent with previous reports (Chahine et al., 1996). The protocols used in this study utilized a uniform period of recording time between 2 to 10 min, therefore time-dependent shift on average were less than 2 mV. To further minimize this time-dependent shift of the voltage dependence of steady-state activation and inactivation, sodium currents from control and drug-pretreated cells were uniformly recorded 10 min after breaking the seal, the period which shows the largest shift after breaking the membrane.

Voltage protocols used for steady-state activation and inactivation of whole-cell recording and single channel recording are described in detail in the figure legends. Whole-cell peak current from both channel isoforms ranged from 0.8 to 3.5 nA ($I_{Na,\ hH1a}$ = 1.86 ± 0.24, n = 9; $I_{Na,\ \mu l}$ = 1.89 ± 0.21, n = 17); larger whole-cell currents were discarded. For whole-cell recording, the following criteria were used as a measure of adequate voltage control: (i) the mean slope for steady-state activation of hH1a and μl transfected in control HEK293 cells were 6.16 ± 0.40 (n = 9) and 6.23 ± 0.14 (n = 17), and any recording with a slope smaller than 5.5 was discarded; (ii) the time to peak current for the test pulse of steady-state inactivation must be the same; and (iii) small cells, with no processes, and with round or spindle-liked shapes were used. Effects of series resistance on the membrane potential were minimized by limiting analysis to those recordings in which uncompensated series resistance contributed less than a 1.5 mV error. The maximum series resistance (Rs) is 0.4 MΩ and the maximum voltage error (V_{error}) is 1.4 mV. No corrections were made for liquid junction potentials. The standard holding potential for all of the pulse protocols was −120 mV. Experiments were carried out at room temperature (22–25°C).

Data Analysis

Patch-clamp data were analyzed using a combination of pCLAMP software (Axon Instruments), Origin (Microcal™ Software) and a custom program written and supplied by David Piper (Webfoot software, University of Utah, Salt Lake City). For statistical analysis of the data, student's unpaired *t*-test or one-way ANOVA together with post-hoc test were used. All P values were significant at 0.05 level or better. Data are presented as mean ± SEM.

Results

Steady-State Activation and Inactivation of hH1a and μl Expressed in Control HEK293 Cells

In identical mammalian expression systems under identical conditions the voltage dependence of steady-state activation and inactivation is shifted in the hyperpolarized direction for the cardiac Na channel (hH1a) relative to the adult skeletal muscle channel (μl). Figure 1*A* shows the current traces for hH1a and μl heterologously expressed in control HEK293 cells. The current-voltage relationships of control hH1a and μl are shown in Fig. 1*B*. hH1a starts to activate around −75 mV, in contrast μl starts to activate at about −50 mV. The mean peak currents for hH1a and μl were 1.86 ± 0.24 (n = 9) and 1.89 ± 0.21 (n = 17). The values of midpoint voltage ($V_{1/2}$) and slope for steady-state activation of either hH1a or μl were obtained from fitting the conductance-voltage curve with the Boltzmann equation. The $V_{1/2}$ and slope for steady-state activation of hH1a are −47.8 ± 1.3 mV and 6.2 ± 0.4 (n = 9), and for μl are −28.3 ± 0.9 mV and 6.2 ± 0.2 (n = 17), respectively. For steady-state inactivation of hH1a and μl transfected in control HEK293 cells (Fig. 2), the data for midpoint voltage ($V_{1/2}$) and slope in both channel isoforms were obtained from Boltzmann fits of steady-state inactivation curves. The $V_{1/2}$ and slope for steady-state inactivation of hH1a are −92.4 ± 2.4 mV and 6.1 ± 0.3 (n = 9), and −70.7 ± 0.8 mV and 6.2 ± 0.3 (n = 17) for μl. These values for $V_{1/2}$ and slope for steady-state activation and inactivation of control hH1a and μl are similar to previous data (Chahine et al., 1996; Satin et al., 1992; Wang, George & Bennett, 1996). The $V_{1/2}$ values for both steady-state activation and inactivation of control hH1a from this study were shifted in the hyperpolarizing direction by about 20 mV relative to those of μl.

Deglycosylation of Sodium Channels with Either Glycosidase or Enzyme Inhibitor Causes Depolarizing Shifts of Steady-State Activation for both hH1a and μl

To test whether sialic acid residues affect the voltage dependence of channel gating, we pretreated cells with

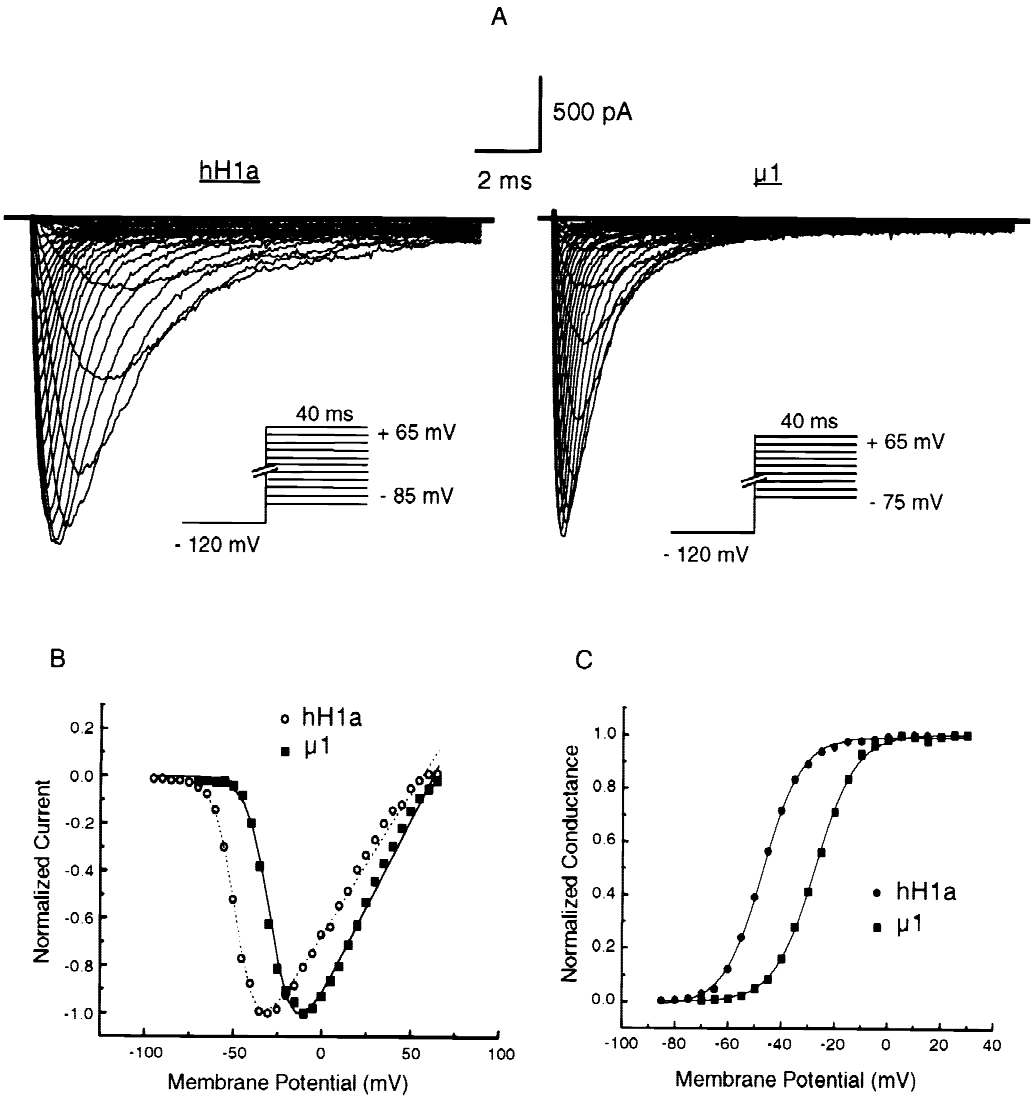

Fig. 1. (*A*) Steady-state activation of hH1a and μl transfected in HEK293 cells under control condition. Left: hH1a. Right: μl. Currents were elicited by a 40-msec depolarizing pulse to potentials ranging from −85 to +65 mV for hH1a and from −75 to +65 mV for μl in 5 mV intervals from the −120 mV holding potential. The interpulse interval was 1.5 sec. (*B*) Whole-cell current-voltage relationship for hH1a and μl. The *I-V* curves were constructed by plotting the peak currents shown in Fig. 1*A* against the membrane potentials. Open circle: hH1a. Solid square: μl. (*C*) Steady-state conductance (G) −voltage (V) relationship of hH1a and μl. Square: μl. Circle: hH1a. The steady-state *G-V* data were transformed from *I-V* data in Fig. 1*B* based on the equation $G = I/(V\text{-}V_{rev})$, where G is conductance and V_{rev} is reversal potential. The solid and dotted curves are fits of the data to the Boltzmann equation of the form: $G/G_{max} = 1/(1 + \exp(V_{1/2} - V)/k)$, where G_{max} is maximum conductance, $V_{1/2}$ is midpoint voltage, and k is the slope. The $V_{1/2}$ and slope from Boltzmann fits of pooled steady-state activation of hH1a and μl are shown in Table.

the exoglycosidase neuraminidase to remove sialic acid, or with castanospermine and swainsonine to prevent the addition of sugar residues to either hH1a or μl sodium channels. Removal of negatively charged sugar residues on the extracellular face of sodium channels by deglycosylation reduces the surface potential. If the voltage sensor is influenced by the electric field created by sugar residues we should observe a depolarizing shift for the voltage dependence of channel activation following deglycosylation. In hH1a transfected cells, the steady-state activation curves for control, castanospermine, swainsonine, and neuraminidase-pretreated groups are shown in Fig. 3*A*. The mean $V_{1/2}$ values and slopes obtained from Boltzmann fits of steady-state activation data are indicated in the Table. Castanospermine, swainsonine, and neuraminidase pretreatment caused a significant depolarizing shift of $V_{1/2}$ for steady-state activation of hH1a from −47.8 ± 1.3 mV ($n = 9$) of control to −40.9 ± 0.8 ($n = 8$), −40.0 ± 0.6 ($n = 8$) and −39.0 ± 0.5 ($n = 6$) mV, respectively, a ΔV ranging from 7 to 9 mV (Table). However, pretreatment with these enzymes did not cause a significant change in the slope of steady-state activation for hH1a (Table).

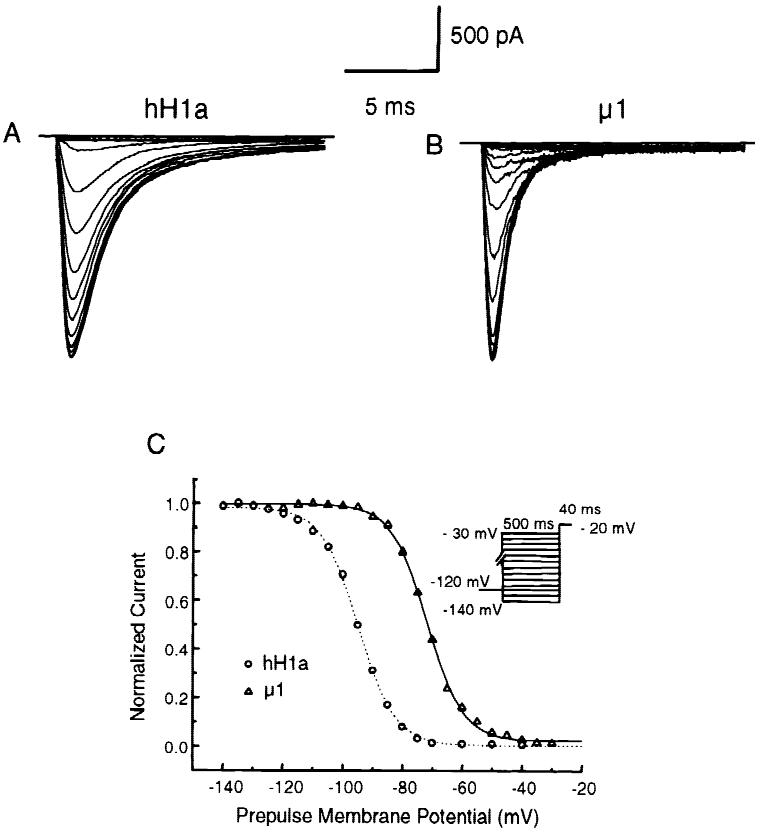

Fig. 2. Voltage dependence of sodium channel availability (steady-state inactivation) for hH1a and μl transfected in HEK293 cells under control condition. (*A and B*) Current traces of steady-state inactivation of hH1a and μl. The steady-state inactivation was obtained using a double pulse protocol from holding potential of −120 mV. The membrane potential was changed to the level displayed on the abscissa for a period of 500 msec. Subsequently, the membrane potential was stepped to −20 mV for 40 msec; the interpulse time was 10 sec. (*C*) Steady-state inactivation curves of hH1a and μl. Open circle: hH1a. Open triangle: μl. The dotted and solid lines through data points are fits of the data to single Boltzmann distributions, $I/I_{max} = \{1 + \exp(V - V_{1/2})/k\}^{-1}$. The $V_{1/2}$ and slope for Boltzmann fits of pooled steady-state inactivation data are shown in the Table.

Table. Comparison of the steady-state parameters for hH1a and μl transfected in HEK293 cell

Cells	No. of cells	Steady-state activation		Steady-state inactivation	
		$V_{1/2}$ (mV)	Slope (mV)	$V_{1/2}$ (mV)	Slope (mV)
Control hH1a	9	−47.8 ± 1.3	6.2 ± 0.4	−92.4 ± 2.0	6.1 ± 0.3
Castanospermine-treated hH1a	8	−40.9 ± 0.8***	6.3 ± 0.1	−81.8 ± 0.7**	6.4 ± 0.3
Swainsonine-treated hH1a	8	−40.0 ± 0.6***	6.2 ± 0.2	−81.2 ± 0.5***	6.3 ± 0.3
Neuraminidase-treated hH1a	6	−39.0 ± 0.5***	6.0 ± 0.2	−80.4 ± 1.7**	6.1 ± 0.4
Control μl	17	−28.3 ± 0.9	6.2 ± 0.2	−70.7 ± 0.8	6.2 ± 0.3
Castanospermine-treated μl	11	−19.4 ± 0.8***	7.6 ± 0.2***	−74.3 ± 1.1**	6.3 ± 0.2
Swainsonine-treated μl	9	−19.5 ± 0.9***	7.1 ± 0.2**	−75.1 ± 1.7*	6.3 ± 0.3
Neuraminidase-treated μl	7	−20.7 ± 1.4***	7.5 ± 0.4***	−74.9 ± 1.6*	6.3 ± 0.4

Values are the Mean ± SEM of the parameters described for each group. Groups pretreated with different glycosidases were compared with the control group for corresponding sodium channel isoform to test significance as follows: *** $P < 0.001$; ** $P < 0.01$; *$P < 0.05$.

Similar to hH1a, Fig. 3*B* shows the steady-state activation curves for control, and various drug-pretreated μl. The pooled values of $V_{1/2}$ and slope for steady-state activation of control and deglycosylated μl acquired from Boltzmann fits are indicated in the Table. Pretreatment with castanospermine, swainsonine, or neuraminidase caused a depolarizing shift of $V_{1/2}$ for steady-state activation of μl ranging from 7.6 to 9.0 mV (Table). In contrast to the effect of deglycosylation on the slope of the steady-state activation of hH1a, deglycosylation of μl with different drug treatments induced a significant reduction of the steepness of steady-state activation, reflected as the increase in the slope values of steady-state activation (Table).

High External Divalent Cation Concentration Masks the Deglycosylation-Induced Depolarizing Shift for Steady-State Activation

Increased extracellular concentration of divalent cations (e.g., Ca^{2+} and Mg^{2+}, etc.) elicits a depolarizing shift of

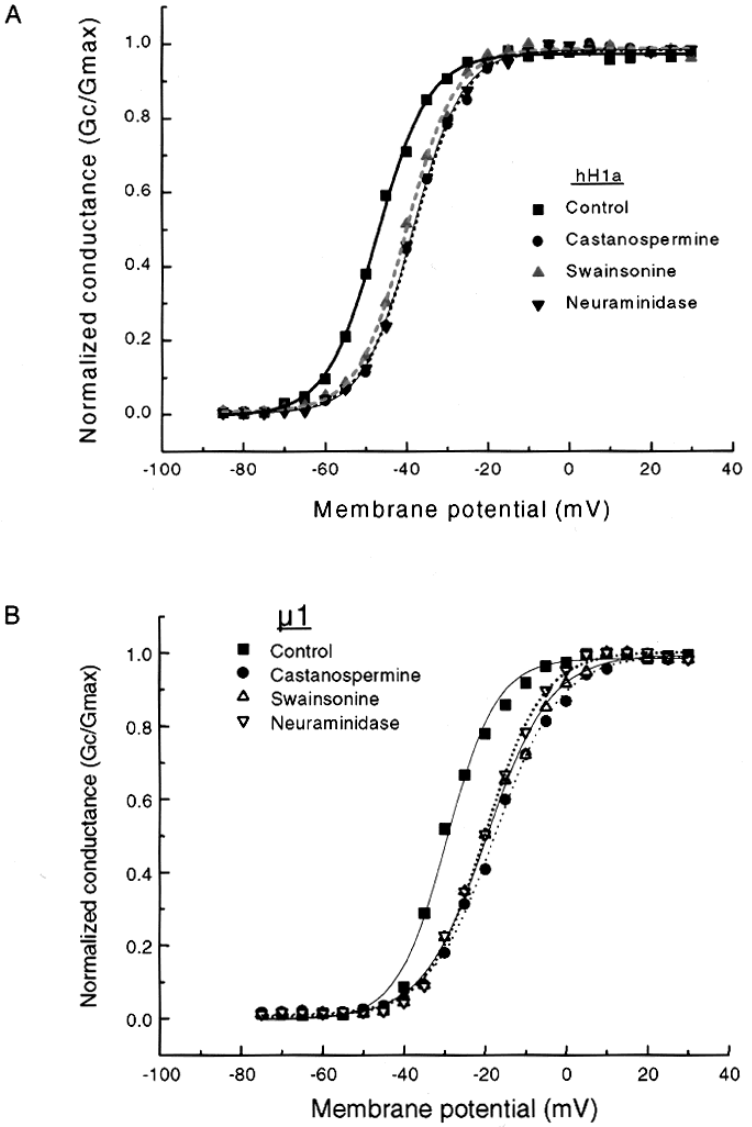

Fig. 3. Deglycosylation with enzyme inhibitors or glycosidase affects the steady-state activation of hH1a and μl transfected in HEK293 cells. Steady-state *G-V* curves shown in *A* and *B* are fits of the data to the Boltzmann equation: $g/g_{max} = 1/(1 + \exp(V_{1/2} - V)/k)$). The values of $V_{1/2}$ and slope from Boltzmann fits of steady-state activation of pooled control and deglycosylated hH1a or μl are indicated in the Table. (*A*) Deglycosylation caused the depolarizing shift of steady-state activation of hH1a. Solid square: control hH1a. Solid circle: castanospermine-pretreated (100 μg/ml) hH1a. Solid up triangle: swainsonine-pretreated (500 ng/ml) hH1a. Solid down triangle: neuraminidase-pretreated (0.15 U/ml) hH1a. (*B*) Deglycosylation induces a depolarizing shift of steady-state activation of μl. Solid square: control μl. Solid circle: castanospermine-treated (100 μg/ml) μl. Open up triangle: swainsonine-treated (500 ng/ml) μl. Open down triangle: neuraminidase-treated (0.15 U/ml) μl.

the voltage dependence for steady-state activation of sodium channels mainly by screening or binding to the negatively charged sites on the extracellular side of the channel (Hille, Woodhull & Shapiro, 1975; Århem, 1980; Gilly & Armstrong, 1982; Neumcke & Stampfli, 1984; Sheets & Hanck, 1992). Therefore, if the deglycosylation-induced depolarizing shift of the voltage dependence of steady-state activation for either hH1a or μl is due to removal of negative surface charge, addition of an external divalent cation to the recording bath should mask the shifting effects caused by enzymatic deglycosylation. The increased external Mg^{2+} should titrate all the remaining negative surface charge, by binding and/or screening charges (including charged sugar residues). Mg^{2+} in contrast to Ca^{2+}, mainly causes screening effects, though not exclusively, in the concentration range used (Nilius, 1988; Hille, 1992; Sheets & Hanck, 1992). Figure 4 demonstrates that high external Mg^{2+} concentration (10 to 30 mM) significantly masked the castanospermine-induced depolarizing shifts of the midpoint voltage ($V_{1/2}$) for steady-state activation of both hH1a (Fig. 4*A*) and μl (Fig. 4*B*). Also, the sensitivity of channel activation to magnesium shift was shown to be reduced in deglycosylated hH1a or μl. The fact that high Mg^{2+} shifted the $V_{1/2}$ of activation of both control and deglycosylated hH1a and μl suggests the existence of two types of surface charges on the channels, one due to the negatively charged sugar residues, the other that is influenced by Mg^{2+} but not by castanospermine. Nevertheless, the results from Fig. 4 suggest that channel associated sialic acid residues are sites of magnesium screening or binding, and the effect of deglycosylation

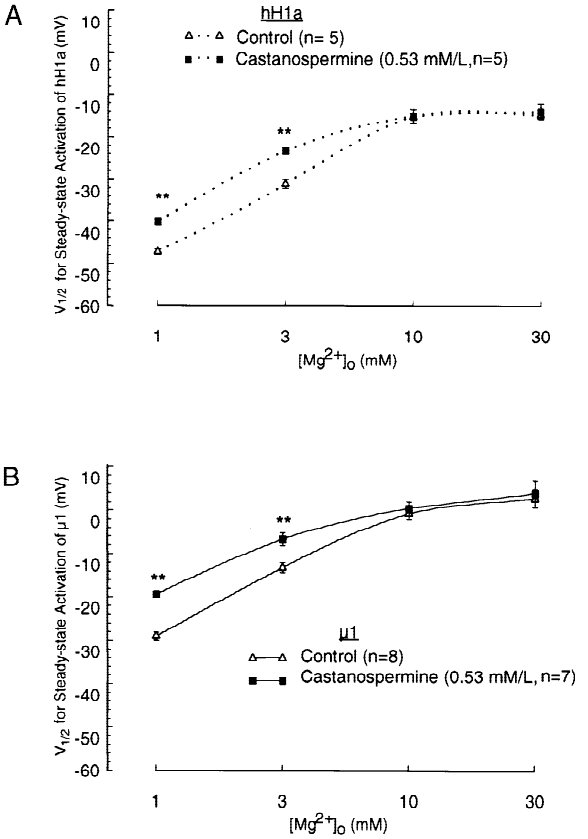

Fig. 4. High extracellular Mg^{2+} concentration diminishes the castanospermine-induced shifts of the midpoint voltage ($V_{1/2}$) for steady-state activation of both hH1a and μl. The $V_{1/2}$ for steady-state activation of either hH1a (*A*) or μl (*B*) is plotted as a function of extracellular Mg^{2+} concentration. Open triangle: control. Solid square: castanospermine (100 μg/ml)–pretreated. $^{**}P < 0.001$ *vs.* control with corresponding extracellular Mg^{2+} concentration. All data are mean ± SEM.

on shifting the voltage dependence of steady-state activation of sodium channels is due to the removal of the negative surface charge contributed by sugar residues.

Removal of Sugar Residues of Sodium Channels Causes Different Effects on Steady-State Inactivation of hH1a and μl

The effect of sugar residues on steady-state inactivation of either hH1a or μl was also determined because the inactivation process is coupled to activation (Armstrong & Bezanilla, 1977; Aldrich, Corey & Stevens, 1983), and to test whether an external field created by sugar residues influences inactivation. Figure 5*A* and *B* are the steady-state inactivation curves for hH1a and μl in both control and deglycosylated-groups. Pretreatment of cells with castanospermine, swainsonine and exoglycosidase neuraminidase elicited about a 10.6 to 12 mV depolarizing shift of midpoint voltage ($V_{1/2}$) in hH1a transfected groups (Table). However, deglycosylation with corresponding drug pretreatment induced a small (ΔV = 3.6 to 4.4 mV), but statistically significant hyperpolarizing shift of $V_{1/2}$ for μl transfected cells (Table). Deglycosylation of sodium channels with glycosidase and enzyme inhibitors had no significant effects on the slope for steady-state inactivation of either hH1a or μl (*see* Table).

The time course of decay of macroscopic current following a depolarization is governed largely by the inactivation process for large depolarizations, and is influenced by the slow kinetics of activation for smaller depolarizations (Aldrich, Corey & Stevens, 1983). We predict that deglycosylation will therefore shift the τ_{decay} of macroscopic current for small depolarizations, via the same charge screening as for activation, but will have no effect for large depolarizations unless inactivation is also affected by glycosylation. hH1a required a bi-exponential fit, as expected for a cardiac Na channel (Fig. 6). In general the fast rate of macroscopic decay was more than two-thirds of the total amplitude. The slow time constant was unaffected by neuraminidase (Fig. 6*A*). In contrast, neuraminidase caused a +10 mV shift of $\tau_{fast,hH1a}$-voltage curve, as well as a slowing of decay kinetics, for hH1a for potentials less than −20 mV (Fig. 6*B*). Similarly, neuraminidase also caused about a +10 mV translation of the tau (*V*) curve and/or slowing of time constants for μl for potentials negative to −20 mV. However, neuraminidase has no effect on hH1a positive to −20 (Fig. 6*B*), while for μl there is some slowing of inactivation in this depolarized range (Fig. 6*C*).

Glycosidase Exerts no Significant Effects on Single-Channel Conductance, Mean Open Time and Open Probability

Recio-Pinto et al. (1990) reported that neuraminidase treatment elicited an increase in the frequency of reversible transitions to subconductance states of electroplax sodium channels in planar lipid bilayer. This suggests that removal of negatively charged sugar residues on sodium channels may cause discrete conformational changes in the channel protein, and such an instability of protein structure might affect the conductance or gating behavior at the single channel level. Therefore, we investigated the possible effects of neuraminidase pretreatment on the single-channel properties including the conductance, the mean open time, and the open probability of μl. Figure 7*A* shows that neuraminidase pretreatment did not significantly change the single channel conductance of μl, from 26.1 pS in control to 27.0 pS in neuraminidase-pretreated groups. Similarly, neuraminidase-pretreated μl and control μl demonstrated the same mean open times at test potentials of −60, −40, −20, or 0 mV

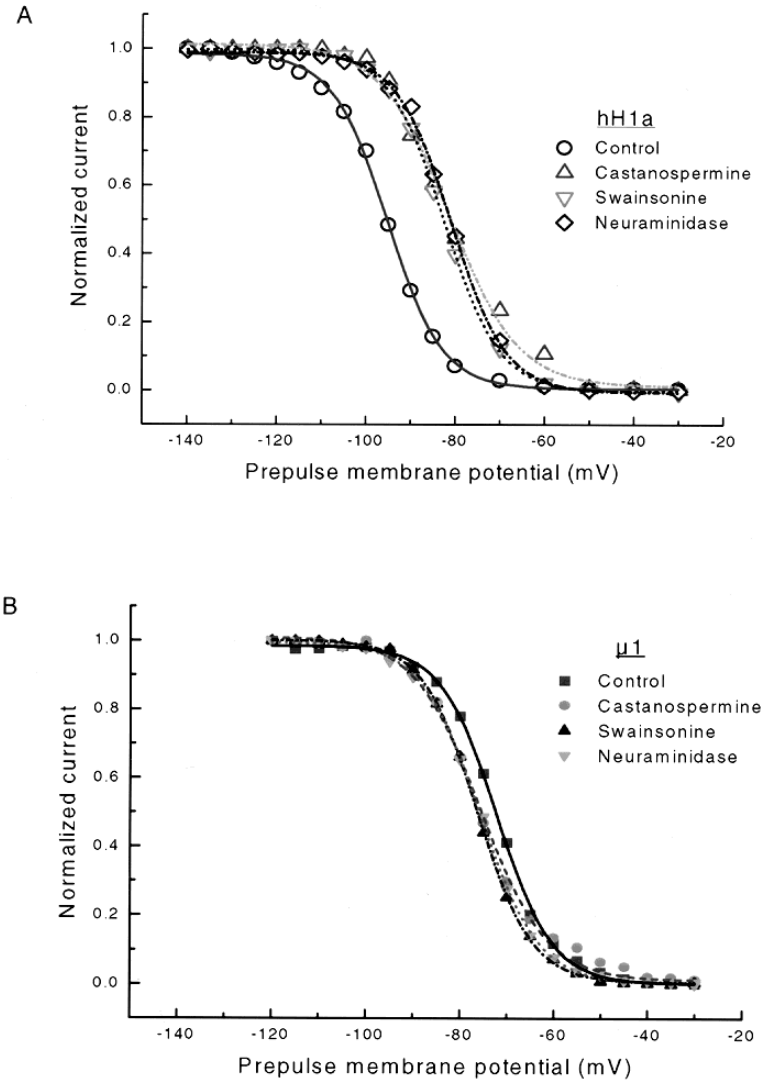

Fig. 5. Removal of sugar residues with glycosidase and enzyme inhibitors causes different effects on steady-state inactivation of hH1a and μl. Steady-state inactivation curves in *A* and *B* are fits of the data to single Boltzmann distributions as described in Fig. 2. The values of $V_{1/2}$ and slope from Boltzmann fits of steady-state inactivation of pooled control and deglycosylated hH1a or μl are shown in the Table. (*A*) Deglycosylation causes a depolarizing shift of steady-state inactivation of hH1a. Circle: control hH1a. Up triangle: castanospermine (100 μg/ml)-pretreated hH1a. Down triangle: swainsonine (500 ng/ml)-pretreated hH1a. Diamond: neuraminidase (0.15 U/ml)-pretreated hH1a. (*B*) Deglycosylation elicits the hyperpolarizing shift of steady-state inactivation of μl.

(Fig. 7*B*). The nP_o histories from patches of control μl and neuraminidase-pretreated μl (Fig. 7*C*) indicate that neuraminidase treatment did not exert a significant change in the single channel open probability (P_o). In addition, the similar shapes of cumulative nP_o from control and neuraminidase-pretreated μl (Fig. 7*D*) suggest that neuraminidase did not induce alternative gating modes. In summary, these data suggest that removal of sugar residues on μl sodium channels has no effect on conductance or permeation properties and does not cause a global disruption of channel conformation.

Discussion

In this study, we transfected cloned human cardiac (hH1a) and rat skeletal muscle (μl) sodium channels into a mammalian cell line to evaluate the effects of sugar residues on voltage-dependent channel gating. Despite the large difference in overall glycosylation of cardiac vs. skeletal muscle Na channels, removal, or impairment of addition of the sugar residues have similar acute effects on most biophysical properties of cardiac and skeletal muscle sodium channels. Our results show that: (i) deglycosylation with either glycosidase or enzyme inhibitor causes a similar, significant depolarizing shift of steady-state activation for both hH1a and μl; (ii) the effect of deglycosylation on steady-state activation of the sodium channel is consistent with a surface charge screening mechanism, alternatively, may be due to electrostatic interaction with a Mg^{2+} binding site; (iii) removal of sugar resides induced different effects on steady-state inactivation for hH1a and μl. Deglycosylation elicted a significant depolarizing shift of steady-state inactivation for hH1a transfected cells, while there was a small but significant hyperpolarizing shift of steady-state inactivation in μl transfected cells. Neuraminidase also slowed the voltage-independent macroscopic inac-

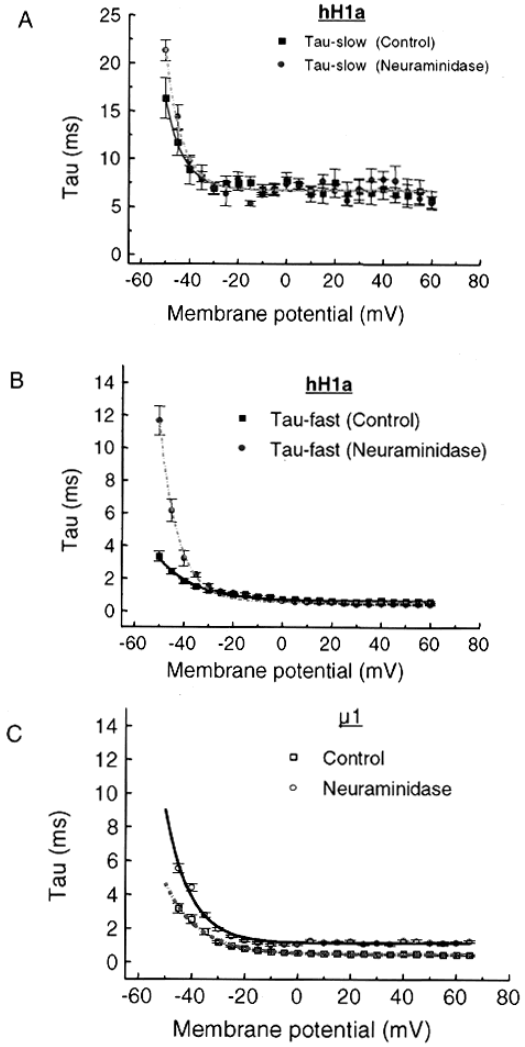

Fig. 6. Neuraminidase shifts voltage dependence of current decay and has isoform-specific effects on voltage-independent macroscopic inactivation. hH1a required a bi-exponential function; in contrast, μl was well fitted by a single exponential. (*A*) Slow time constant of hH1a is unaffected by neuraminidase. (*B*) Neuraminidase shifts $\tau_{fast}(V)$ of hH1a current, but has no effect on voltage-independent phase (>−20 mV). (*C*) Neuraminidase shifts $\tau(V)$ of μl current about 10 mV, and also slows the voltage-independent macroscopic inactivation.

tivation for μl, but not for hH1a; and (iv) neuraminidase had no significant effect on the single channel conductance, the mean open time, and the open probability. In summary, we propose that the major functional effect of sugar residues is to provide surface potential for activation for all Na channel isoforms. However, isoform-specific interactions exist between sugar residues and inactivation gating.

We show that deglycosylation of both cardiac and skeletal muscle sodium channels with either enzyme inhibitors or glycosidase caused significant depolarizing shifts of midpoint voltage for steady-state activation.

Castanospermine and swainsonine inhibit two specific oligosaccharide-processing enzymes which act at early and late steps, respectively, in the processing pathway of N-linked glycosylation. Specifically, castanospermine inhibits glucosidases I and II of the endoplasmic reticulum (Tulsiani & Touster, 1983), and swainsonine inhibits mannosidase II of Golgi (Tulsiani & Touster, 1985). The manipulation with these two enzyme inhibitors interrupts the pathway that leads to further processing, including the sialylation of N-linked oligosaccharide chains.

Castanospermine prevents incorporation of approximately 81% of the sialic acid of native rat brain sodium channel II (Schmidt & Catterall, 1987). The exoglycosidase neuraminidase was also used to specifically remove negatively charged sialic acid residues (James & Agnew, 1987). In the present study, either the castanospermin and swainsonine, or the neuraminidase pretreatment elicited comparable 7 to 9 mV depolarizing shifts of the steady-state activation curve for hH1a and μl, respectively. The consistent effects of different treatments on shifting the voltage dependences of activation curves suggest that various drugs used modified channels through the same mechanism. One possibility for such a common effect is that all these agents act by uniformly desialylating the transfected sodium channels.

Sugar Residues Affect the Voltage Dependence of Channel Activation Through a Surface Charge Mechanism

We tested the hypothesis that negative surface charge contributes to the deglycosylation-induced depolarizing shift of voltage dependent activation. Although there may be more than a single mechanism underlying the effects of deglycosylation on the depolarizing shift of channel activation for both sodium channel isoforms studied, our data support a major role for a surface charge mechanism by sugar residues. Surface charge screening or binding is manifested as a shift of the voltage-dependent activation curve (Frankenhaeuser & Hodgkin, 1957). Briefly, an external field established by charges near the voltage sensor will bias the voltage sensed by the voltage sensor (reviewed by Hille, Woodhull & Shapiro, 1975). Our data show a significant shift of activation midpoint that can be masked by high concentrations of external divalent cations (Mg^{2+}). Also, removal of charged sugar residues reduced the sensitivity of channel activation to magnesium shifts. We suggest that sugar residues provide such a cloud of negative surface charge. Deglycosylation reduces the bias voltage by removing negatively charged sugar residues. Implicit in this argument is the assumption that the voltage-sensing domains are biased by the potential drop from the sugars.

Structure-function studies have shown that the S4 (fourth transmembrane α-helical segment) is largely responsible for voltage sensing (Stühmer et al., 1989; Yang & Horn, 1995). The outer charges of S4 are predicted to move out of the membrane upon activation (Mitrovic, George & Horn, 1998). We speculate that such an S4 movement may move S4 charges through the electric field created by sugar residues. In conditions of high divalent cation concentration the negative charges are screened or bound so that there is no apparent effect of sugars. At physiological cation concentrations, however, sugar residues electrostatically influence voltage sensing.

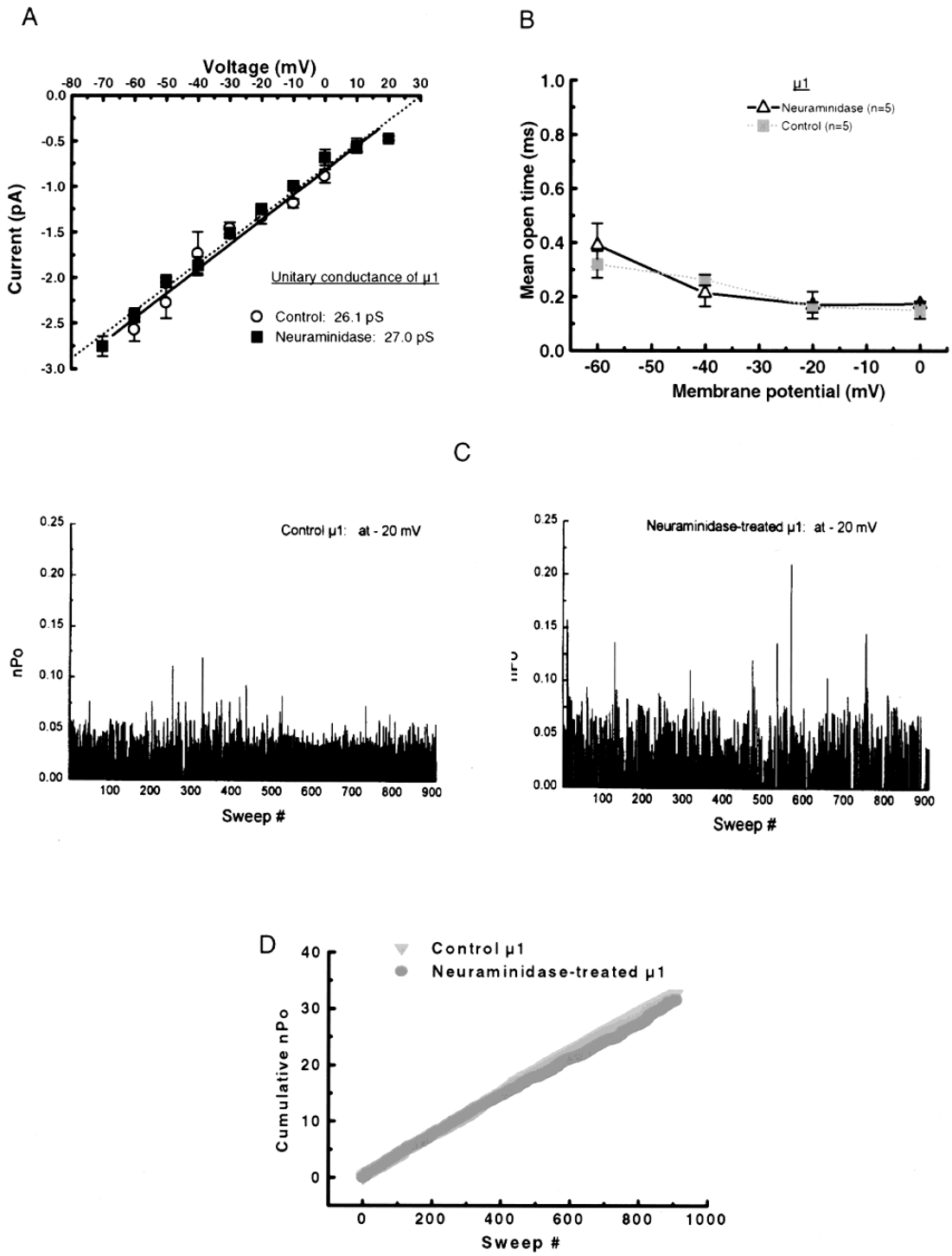

Fig. 7.

Comparison of Effects of Sugar Residues on the Voltage Dependence for Heart Compared to Skeletal Muscle Channels: Isoform Specific Effects on Inactivation

The absolute depolarizing shift of steady-state activation $V_{1/2}$ elicited by deglycosylation is almost the same for μl as that for hH1a. *A priori* we expected a greater effect of deglycosylation on steady-state activation for μl because biochemical studies showed that the cardiac sodium channel carries less carbohydrates compared to noncardiac isoforms (Cohen & Barchi, 1993). Sugar residues account for about 5% of the weight of cardiac sodium channel (Cohen & Barchi, 1993) but almost 20–30% of the mass of noncardiac sodium channel isoforms (Messner & Catterall, 1985). Thus, isoform-specific differences in the physical relationship between sugar residues and the channel structure, which helps to sense the change in the electrical field elicited by deglycosylation, may explain the same degree of $V_{1/2}$ shift for activation of μl and hH1a pretreated with glycosidase and enzyme inhibitors.

In contrast to steady-state activation, the response to deglycosylation of steady-state inactivation was dramatically different for heart compared to the skeletal muscle channel. As expected from a reduction of negative surface potential the cardiac inactivation curve was shifted 11 mV positive, similar to the shift of the activation curve. Similarly, the approximate +10 mV shift of the macroscopic decay time constant as a function of voltage is consistent with negatively charged sugar residues constituting part of the total surface charge. The only assumption is that the effect of reduced surface potential on activation is translated to the measured channel availability via the well-established activation-inactivation charge coupling (Maltsev & Undrovinas, 1997). In contrast, the effects of sugar residues on μl were more complex. The skeletal muscle channel inactivation curve was slightly but significantly shifted about 4 mV in the opposite direction from the activation curve. This hyperpolarizing shift of the voltage dependence of inactivation for μl cannot be explained by a direct electrostatic effect via removal of the negative external surface potential. In distinction to the cardiac Na channel, the voltage independent slowing of macroscopic inactivation of μl suggests that neuraminidase has a direct effect on skeletal muscle Na channel inactivation.

Our study is the first to compare the contribution of sugar residues to gating of two different sodium channel isoforms expressed in the identical cell line. In a previous study of μl, deglycosylation by neuraminidase had no effect on the inactivation midpoint. In contrast, expression of μl in a sialylation defective cell resulted in a small depolarizing shift of inactivation. In our study, three different treatments had the same effects on each isoform tested. Our μl results differ from Bennett et al. (1997) for reasons that are unclear. Several differences in detail between our studies may contribute to such a difference including the composition of the intracellular solution. We avoided CsF because we have noted an erratic time-dependent shift of voltage dependencies in contrast to F^--free internal solutions. Also, under control conditions the slope factor for the activation curve for μl in our study (6.18 ± 0.27) was less steep than that in Bennett et al. (5.68 ± 0.36). This margin constituted a significant difference in the earlier study and may indicate poorer voltage control. In any case, the isoform-specific modulation of inactivation that we demonstrate is intriguing and is consistent with fundamental differences in activation-inactivation coupling.

Other Mechanisms Possibly Involved in Effects of Sugar Residues on Sodium Channel Gating

Our data indicate that enzymatic deglycosylation of μl with neuraminidase has no effect on single channel conductance, appearance of subconductance states, or mean open time. Furthermore, we found no evidence that additional modes of channel gating are induced by deglycosylation. These data support the argument that deglycosylation does not alter conductance properties, nor does it seem to globally change channel properties.

Fig. 7. Effects of neuraminidase on single channel kinetics of μl. (*A*) Single-channel current-voltage relationship for μl. Open circle: control μl ($n = 5$). Solid square: neuraminidase (0.15 U/ml)-treated μl ($n = 5$). Single channel openings were measured with depolarizing steps to different membrane potentials indicated in Fig. 7*A* for hundreds of sweeps for each step from the holding potential of −120 mV. The duration for each depolarizing step and the interpulse time between the sweeps were 40 msec and 1.5 sec. The *I-V* curves are fits of single channel amplitudes under different membrane potentials to linear least-squares. All data are mean ± SEM. (*B*) Effects of neuraminidase on mean open time (MOT) of single channel μl at different test potential. Solid: control μl ($n = 5$). Open triangle: neuraminidase (0.15 U/ml)–treated μl ($n = 5$). The open time histograms under both control and neuraminidase-pretreated conditions were best fit with single exponential, resulting in MOTs (tau) at −60, −40, −20, and 0 mV for both groups. Data are mean ± SEM. No significance was found for MOTs at each test potential between two groups. (*C*) nP_o histories from representative patches of control μl and neuraminidase-pretreated μl. Left panel: control. Right panel: neuraminidase (0.15 U/ml)-treated. Single channel events were −1.39 pA and −1.33 pA, respectively. A maximum of three overlapping events were detected in 910 sweeps for either control or neuraminidase-pretreated patch with depolarizing step to −20 mV. The test protocol was same as that described in Fig. 7*A*. (*D*) Cumulative nP_o from representative patches of control μl and neuraminidase-pretreated μl. Triangle line: control. Circle line: neuraminidase (0.15 U/ml)-pretreated. The representative patches are corresponding to those indicated in Fig. 7*C*, and the test protocol was same as that described in Fig. 7*A*.

Removal of sugar residues reduces the steepness of the slope for steady-state activation over the entire activation range (Table), as well as for the slope in the moderate activating range of potentials (Fig. 3). This reduction in the steepness of slope of steady-state activation reflects the intrinsic changes in the effective valence of gating charges within a voltage sensor (Hille, 1992). However, the change in the slope for steady-state activation is complex and although it is partially influenced by gating charge movement, the steady-state activation slope is biased by the share of energy required for conformational changes leading to ionic permeation, and it may be also influenced by cooperative transitions of gating structures (Schoppa et al., 1992; Sheets & Hanck, 1992).

The results from our study and from Bennett and colleagues (1997) are in contrast to a previous study on electroplax Na channels studied in lipid bilayers (Recio-Pinto et al., 1990) where neuraminidase led to dispersion of the activation curve and multiple sublevels. Although on an evolutionary scale eel and mammals are far apart we suggest that the discrepancy between our data and the bilayer study stems from the use of batrachotoxin (BTX) in their study. BTX causes persistent activation of a variety of Na channels (Khodorov, 1985). BTX itself can affect channel gating, including eliciting the multiconductance states and change in the mean open time of single sodium channels (Green, Weiss & Andersen, 1987; Tanguy & Yeh, 1988). Hence, we suggest that it is difficult to sort out super-imposed BTX and glycosidase induced modifications based on data from that lipid bilayer study. Our data support the hypothesis that sugar residues may dynamically modulate Na current by providing an external potential drop.

Voltage sensing is a fundamental properties of all voltage-gated ion channels. The potential physiological importance of sugar residues on sodium channel gating may be in its regulating the voltage dependence of channel activation and inactivation. Because of the steepness of curves for steady-state activation and inactivation in cardiac and skeletal muscle sodium channels, small shifts of voltage dependence for activation and inactivation can dramatically alter the fraction of channels available to open, or alter the probability that a channel opens. We conclude, that by creating an external potential drop post-translationally added acidic sugar residues may modulate Na channel function.

This work was supported by an American Heart Association National Center Grant-in-Aid.

References

Aldrich, R.W., Corey, D.P., Stevens, C.F. 1983. A reinterpretation of mammalian sodium channel gating based on single channel recording. *Nature* **306:**436–441

Århem, P. 1980. Effects of some heavy metal ions on the ionic currents of myelinated fibres from *Xenopus laevis*. *J. Physiol.* **306:**219–231

Armstrong, C.M., Bezanilla, F. 1977. Inactivation of the sodium channel: II. Gating current experiments. *J. Gen. Physiol.* **70**(5):567–590

Barchi, R.L., Cohen, S.A., Murphy, L.E. 1980. Purification from rat sarcolemma of the saxitoxin-binding component of the excitable membrane sodium channel. *Proc Natl. Acad. Sci., USA* **77:**1306–1310

Bennett, E., Urcan, M.S., Tinkle, S.S., Koszowski, A.G., Levinson, S.R. 1997. Contribution of sialic acid to the voltage dependence of sodium channel gating: A possible electrostatic mechanism. *J. Gen. Physiol.* **109:**327–343

Bradshaw, R.A., McAlister-Henn, L., Douglas, M.G. 1988. *Molecular Biology of Intracellular Protein Sorting and Organelle Assembly.* Alan R. Liss, New York

Catterall, W.A. 1992. Cellular and molecular biology of voltage-gated sodium channels. *Physiol. Rev.* **72:**S15–S48

Chahine, M., Bennett, P.B., George, A.L., Jr., Horn, R. 1994. Functional expression and properties of the human skeletal muscle sodium channel. *Pfluegers. Arch.* **427:**136–142

Chahine, M., Deschene, I., Chen, I.Q., Kallen, R.G. 1996. Electrophysiological Characteristics of Cloned Skeletal and Cardiac Muscle Sodium Channels. *Am. J. Physiol.* **271:**498–506

Cohen, S.A., Barchi, R.L. 1993. Voltage-dependent sodium channels. *Int. Rev. Cytol.* **137C:**55–103

Cohen, S.A., Levitt, L.K. 1993. Partial characterization of the rH1 sodium channel protein from rat heart using subtype-specific antibodies. *Circ. Res.* **73:**735–742

Elmer, L.W., O'Brien, B.J., Nutter, T.J., Angelides, K.J. 1985. Physicochemical characterization of the alpha-peptide of the sodium channel from rat brain. *biochem* **24:**8128–8137

Fermini, B., Nathan, R.D. 1991. Removal of sialic acid alters both T-type and L-type calcium currents in cardiac myocytes. *Am. J. Physiol.* **260:**(3)H735–743

Frankenhaeuser, B., Hodgkin, A.L. 1957. The action of calcium on the electrical properties of squid axons. *J. Physiol.* **137:**218–244

Gellens, M.E., George, A.L., Chen, L.Q., Chahine, M., Horn, R., Barchi, R.L., Kallen, R.G. 1992. Primary structure and functional expression of the human cardiac tetrodotoxin-insensitive voltage-dependent sodium channel. *Proc. Natl. Acad. Sci., USA* **89:**554–558

Gilly, W.F., Armstrong, C.M. 1982. Slowing of sodium channel opening kinetics in squid axon by extracellular zinc. *J. Gen. Physiol.* **79:**935–964

Gordon, D., Merrick, D., Wollner, D.A., Catterall, W.A. 1988. Biochemical properties of sodium channels in a wide range of excitable tissues studied with site-directed antibodies. *Biochem* **27:**7032–7038

Green, W.N., Weiss, L.B., Andersen, O.S. 1987. Batrachotoxin-modified sodium channels in planar lipid bilayers: Ion permeation and block. *J. Gen. Physiol.* **89:**841–872

Hanck, D.A., Sheets, M.F. 1992. Extracellular divalent and trivalent cation effects on sodium current kinetics in single canine cardiac Purkinje cells. *J. Physiol.* **454:**267–298

Hille, B. 1992. *Ionic Channels of Excitable Membranes.* Sinauer Associates, Sunderland, MA

Hille, B., Woodhull, A.M., Shapiro, B.I. 1975. Negative surface charge near sodium channels of nerve: divalent ions, monovalent ions, and pH. *Philos. Trans. Roy Soc Lond. B* **270:**301–318

James, W.M., Agnew, W.S. 1987. Multiple oligosaccharide chains in the voltage-sensitive Na channel from electrophorus electricus: evidence for alpha-2,8-linked polysialic acid. *Biochem. Biophys. Res. Commun.* **148:**817–826

Khodorov, B.I. 1985. Batrachotoxin as a tool to study voltage-sensitive

Na channels of excitable membrane. *Prog. Biophys. Molec. Biol.* **45:**57–148

Maltsev, V.A., Undrovinas, A.I. 1997. Cytoskeleton modulates coupling between availability and activation of cardiac sodium channel. *Am. J. Physiol.* **273:**1832–1840

Matter, K., Mellman, I. 1994. Mechanisms of cell polarity: Sorting and transport in epithelial cells. *Current Opinion in Cell Biology* **6:**545–554

Messner, D.J., Catterall, W.A. 1985. The sodium channel from rat brain: separation and characterization of subunits. *J. Biol. Chem.* **260:**10597–10604

Miller, J.A., Agnew, W.S., Levinson, S.R. 1983. Principal glycoprotein of the tetrodotoxin/saxitoxin binding proteins from *Electrophorus electricus:* isolation and partial chemical and physical characteristics. *Biochem* **22:**462–470

Mitrovic, N., George, A.L., Horn, R. 1998. Independent versus coupled inactivation in sodium channels: Role of the domain 2 S4 segment. *J. Gen. Physiol.* **111:**451–462

Neumcke, B., Stampfli, R. 1984. Heterogeneity of external surface charges near sodium channels in the nodal membrane of frog nerve. *Pfluegers Arch.* **401:**125–131

Nilius, B. 1988. Calcium block of guinea pig heart sodium channels with and without modification by the piperazinylindole DPI 201-206. *J. Physiol.* **399:**537–558

Recio-Pinto, E., Thornhill, W.B., Duch, D.S., Levinson, S.R., Urban, B.W. 1990. Neuraminidase treatment modifies the function of electroplax sodium channels in planar lipid bilayers. *Neuron* **5:**675–684

Satin, J., Kyle, J.W., Chen, M., Rogart, R.B., Fozzard, H.A. 1992. The cloned cardiac sodium channel α-subunit expressed in *Xenopus* oocytes show gating and blocking properties of native channels. *J. Membrane Biol.* **130:**11–22

Scheiffele, P., Peranen, J., Simons, K. 1995. N-Glycans as apical sorting signal in epithelial cells. *Nature* **378:**96–98

Schmidt, J.W., Catterall, W.A. 1987. Palmitylation, sulfation, and glycosylation of the alpha-subunit of the Na channel. *J. Biol. Chem.* **262:**13713–13723

Schoppa, N.E., McCormack, K., Tanouye, M.A., Sigworth, F.J. 1992. The size of gating charge in wild-type and mutant shaker potassium channels. *Science* **255:**1712–1715

Sheets, N.F., Hanck, D.A. 1992. Mechanisms of extracellular divalent and trivalent cation block of the sodium current in canine cardiac Purkinje cells. *J. Physiol.* **454:**299–320

Stühmer, W., Conti, F., Suzuki, H., Wang, X., Noda, M., Yahagi, N., Kubo, H., Numa, S. 1989. Structural parts involved in activation and inactivation of the sodium channel. *Nature* **339:**597–603

Tanguy, J., Yeh, J.Z. 1988. Batrachotoxin uncouples gating charge immobilization from fast Na inactivation in squis giant axons. *Biophys. J* **54:**719–730

Trimmer, J.S., Cooperman, S.S., Tomiko, S.A., Zhou, J., Crean, S.M., Boyle, M.B., Kallen, R.G., Sheng, Z., Barchi, R.L., Sigworth, F.J., Goodman, R.H., Agnew, W.S., Mandel, G. 1989. Primary structure and functional expression of a mammalian skeletal muscle sodium channel. *Neuron* **3:**33–49.

Tulsiani, D.R.P., Touster, O. 1983. Swainsonine causes the production of hybrid glycoproteins by human skin fibroblasts and rat liver golgi preparations. *J. Biol. Chem.* **258:**7578–7585

Tulsiani, D.R.P., Touster, O. 1985. Characterization of a novel alpha-D-mannosidase from rat brain microsomes. *J. Biol. Chem.* **260:**13081–13087

Ukomadu, C., Zhous, J., Sigworth, F., Agnew, W.S. 1992. μl Na^+ channels expressed transiently in human embryonic kidney cells: biochemical and biophysical properties. *Neuron* **8:**663–676

Wang, D.W., George, A.L., Bennett, P.B. 1996. Comparison of heterologously expressed human cardiac and skeletal muscle sodium channels. *Biophys. J.* **70:**238–245

West, C.M. 1986. Current ideas on the significance of protein glycosylation. *Molec. Cell. Biochem.* **72:**3–20

Worley, J.F., French, R.J., Pailthorpe, B.A., Krueger, B.K. 1992. Lipid surface charge does not influence conductance or calcium block of single sodium channels in planar bilayers. *Biophys. J.* **61:**1353–1363

Yang, N., Horn, R. 1995. Evidence for voltage-dependent S4 movement in sodium channels. *Neuron* **15:**213–218